THE JOURNAL OF BIOLOGICAL CHEMISTRY VOL. 290, NO. 52, pp. 30843–30854, December 25, 2015


# Hsp90·Cdc37 Complexes with Protein Kinases Form Cooperatively with Multiple Distinct Interaction Sites*

Received for publication, September 21, 2015, and in revised form, October 27, 2015 Published, JBC Papers in Press, October 28, 2015, DOI 10.1074/jbc.M115.693150

**Julia M. Eckl[‡1], Matthias J. Scherr[‡1], Lee Freiburger[‡§2], Marina A. Daake[‡], Michael Sattler[‡§], and Klaus Richter[‡3]**

*From the [‡]Center for Integrated Protein Science München at Department of Chemistry, Technische Universität München, 85748 Garching, Germany and [§]Institute of Structural Biology, Helmholtz Zentrum München, 85764 Neuherberg, Germany*

**Protein kinases are the most prominent group of heat shock protein 90 (Hsp90) clients and are recruited to the molecular chaperone by the kinase-specific cochaperone cell division cycle 37 (Cdc37). The interaction between Hsp90 and nematode Cdc37 is mediated by binding of the Hsp90 middle domain to an N-terminal region of *Caenorhabditis elegans* Cdc37 (CeCdc37). Here we map the binding site by NMR spectroscopy and define amino acids relevant for the interaction between CeCdc37 and the middle domain of Hsp90. Apart from these distinct Cdc37/Hsp90 interfaces, binding of the B-Raf protein kinase to the cochaperone is conserved between mammals and nematodes. In both cases, the C-terminal part of Cdc37 is relevant for kinase binding, whereas the N-terminal domain displaces the nucleotide from the kinase. This interaction leads to a cooperative formation of the ternary complex of Cdc37 and kinase with Hsp90. For the mitogen-activated protein kinase extracellular signal-regulated kinase 2 (Erk2), we observe that certain features of the interaction with Cdc37·Hsp90 are conserved, but the contribution of Cdc37 domains varies slightly, implying that different kinases may utilize distinct variations of this binding mode to interact with the Hsp90 chaperone machinery.**

The human genome encodes up to 500 kinases, which represent one of the largest families of genes in eukaryotes (1, 2). They regulate essential intracellular processes like proliferation, differentiation, development, stress response, and apoptosis. All protein kinases share a conserved catalytic domain, which switches between an active and an inactive state (3, 4). A large number of these protein kinases are dependent on the Hsp90 chaperone system, which modulates their maturation and prevents their degradation (5–8). So far only little structural information of the chaperone-kinase complex is available (9). To facilitate kinase processing by the Hsp90 chaperone machinery, the specific cochaperone Cdc37 is required (9–11). A well described function of this cochaperone is to slow down the ATPase activity of Hsp90 (12). It is widely expected that Hsp90 and its partner protein Cdc37 bind to the catalytic domain of the kinase (13–16). It remains elusive how the ternary complex consisting of protein kinase, Hsp90 and Cdc37 is structurally organized and how the protein kinase is processed by the chaperone system. Recently Cdc37 was observed to compete with nucleotide binding to the kinase domain of B-Raf (17), but the role of Hsp90 in these structures remains enigmatic. Although Hsp90 is essential for ligand binding in case of steroid hormone receptors the role for B-Raf activation is rather unclear (18). B-Raf is mutated in many human cancers and is known to form complexes with Hsp90 and Cdc37 in cell free systems (19). The interaction with the kinase is also weakened *in vivo* in presence of an anticancer drug that disrupts nucleotide binding to Hsp90 (20). Given the recent evolution of Hsp90 as a potential cancer target (21–23), it is important to clarify the mechanism and role of the chaperone/kinase interaction.

The molecular chaperone Hsp90[4] itself is a dimeric protein consisting of three domains: an N-terminal ATP binding domain; a middle domain, which is supposed to be involved in client binding; and a C-terminal dimerization domain (24, 25). ATP binding leads to a rearrangement of the three domains from an open V-shaped conformation to a closed conformation (5, 26, 27). It is thought that client proteins interact with the Hsp90 scaffold to stabilize destabilized conformations (6, 28) and that the conformational changes performed by the ATP-driven conformational cycle of Hsp90 are utilized for this. This is supported by the observation that inhibitors that block ATP turnover by Hsp90 can disrupt the interaction with kinase clients (29–31).

Despite the significant homology within eukaryotic Hsp90 systems, *Caenorhabditis elegans* (CeCdc37) and human Cdc37 (hCdc37) utilize a different primary interaction site on Hsp90 *in vitro* (32, 33). Although the nematode cochaperone interacts with the M-domain of Hsp90, the human homolog preferentially binds to the N-terminal domain, suggesting a potential two-site interaction. With only structural information on the N-terminal binding site of Hsp90 available so far, the organization of the binding site in the *C. elegans* system is unclear to date. Here we localize the interaction site of nematode Cdc37

* This work was supported in part by Deutsche Forschungsgemeinschaft Grants RI1873/1-3 (to K. R.) and SFB1035 (to M. J. S.), the Fonds der chemischen Industrie, the TUM Graduate School's Faculty Graduate Center of Chemistry at the Technische Universität München, and the Center for Integrated Protein Science. The authors declare that they have no conflicts of interest with the contents of this article.

[1] Both authors contributed equally to this work.

[2] Supported by European Molecular Biology Organization Long Term Fellowship ALTF 1255-2011 and a Marie Curie International Incoming Fellowship within the Seventh European Community Framework Programme.

[3] To whom correspondence should be addressed: Center for Integrated Protein Science München and Dept. of Chemistry, Technische Universität München, Lichtenbergstrasse 4, 85748 Garching, Germany. Tel.: 49-89-289-13342; Fax: 49-89-289-13345; E-mail: klaus.richter@richterlab.de.

[4] The abbreviations used are: Hsp90, heat shock protein 90; Cdc37, cell division cycle 37; aUC, analytical ultracentrifugation; CeCdc37, *C. elegans* Cdc37; hCdc37, human Cdc37; CeHsp90, *C. elegans* Hsp90; hHsp90, human Hsp90$\beta$; MANT-ADP, 2′/3′-*O*-(*N*-methylanthraniloyl)adenosine 5′-diphosphate; Hsp90M, middle domain of Hsp90; *CeCdc37, labeled full-length CeCdc37.

with Hsp90 in detail and determine the differences regarding the formation of kinase complexes.

## Experimental Procedures

*Cloning, Protein Expression, and Purification*—hCdc37 and human Hsp90$\beta$ (hHsp90) as well as the *C. elegans* homolog proteins of Cdc37 (CeCdc37, CDC-37, W08F4.8), Hsp90 (CeHsp90, DAF-21, C47E8.5) and all variants thereof were purified as described previously (34, 35). The cDNA of human Erk2 was obtained from Sino Biological (Beijing, China). The pET28b plasmid was used as expression vector with the cDNA subcloned after the N-terminal $His_6$ tag. For expression, transformed BL21-CodonPlus(DE3)RIL cells were grown to an $A_{600}$ of 0.8 at 37 °C. Protein production was induced by adding 1 mM isopropyl 1-thio-$\beta$-D-galactopyranoside. Cells were disrupted in a TS 0.75 cell disruption instrument (Constant Systems Ltd., Northants, UK). The $His_6$-tagged proteins were trapped on a HisTrap FF 5-ml affinity column (GE Healthcare) and eluted with buffer containing 300 mM imidazole. ResourceQ ion exchange chromatography and size exclusion chromatography on a Superdex75 or Superdex200 HiLoad column (both GE Healthcare) were subsequently performed. The quality of each purified protein was confirmed by SDS-PAGE and mass spectrometry on a Bruker UltraFlex III MALDI-TOF instrument.

The stabilized kinase domain of the human B-Raf kinase was expressed, purified, and stored according to protocols described previously (17, 36). B-Raf and Erk2 kinases were stored in 20 mM Tris/HCl, pH 7.5, 50 mM KCl, 0.5 mM EDTA, 5 mM $MgCl_2$, 1 mM DTT, and 1% (v/v) glycerol, and all other proteins were kept in 40 mM HEPES/KOH, pH 7.5, 20 mM KCl, and 1 mM DTT.

*Alignment and Structural Features*—A sequence alignment of the N-terminal human (amino acids 1–133) and nematodal (amino acids 1–128) Cdc37 was performed using the ClustalW2 tool (37). A secondary structure prediction of the same domain was carried out using Jpred 3 with default settings (38).

*ATPase Activity Assays*—The ATP turnover of Hsp90 alone and in the presence of cochaperones was analyzed in ATPase activity assays (39). To this end, an ATP-regenerating system containing pyruvate kinase, phosphoenolpyruvate, NADH, and lactate dehydrogenase (Roche Applied Science) was used. Measurements were performed at 25 or 30 °C using 3 $\mu$M Hsp90 and 10 $\mu$M cochaperone in 40 mM HEPES/KOH, pH 7.5, 20 mM KCl, 1 mM DTT, and 5 mM $MgCl_2$. Reactions were started by adding 2 mM ATP, and the absorbance of NADH was recorded at 340 nm. Background activities were detected after adding the Hsp90-specific inhibitor radicicol (Sigma-Aldrich). The activity of Hsp90 was calculated using the following equation with $\epsilon(NAD^+) - \epsilon(NADH) = -6200\ M^{-1}\ cm^{-1}$.

$$\text{Activity} = \frac{\frac{\Delta A_{340}}{\Delta t} - \left(\frac{\Delta A_{340}}{\Delta t}\right)_{\text{Background}}}{(\epsilon(NAD^+) - \epsilon(NADH)) \cdot c(\text{ATPase})} \quad \text{(Eq. 1)}$$

*Fluorescence Labeling*—Cysteine residues of CeCdc37 or hCdc37 were labeled by adding a 3-fold molar excess of Alexa Fluor 488-$C_5$-maleimide (Invitrogen) to 0.5 mg of protein in a buffer containing 40 mM HEPES/KOH, pH 7.5, and 20 mM KCl. After an incubation time of 1 h at room temperature, the reaction was stopped by adding 20 mM DTT, and free label was separated from the labeled protein on a Superdex 75 HR column (GE Healthcare). The degree of labeling (DOL) was determined by full-length mass analysis on a MALDI-TOF instrument (Bruker) and by UV/visible spectroscopy using the following equations.

$$A_{\text{protein}} = A_{280} - A_{\text{max}} \cdot (CF_{280}) \quad \text{(Eq. 2)}$$

$$\text{DOL} = \frac{A_{\text{max}} \cdot M_r}{[\text{protein}] \cdot \epsilon_{\text{dye}}} \quad \text{(Eq. 3)}$$

The values $CF_{280} = 0.11$ and $\epsilon_{\text{dye}} = 71{,}000\ M^{-1}\ cm^{-1}$ were used according to the manufacturer. The positions of the labels on CeCdc37 were determined using electrospray ionization mass spectrometry on an OrbiTrap XL (Thermo Scientific).

*Mass Spectrometry on Labeled CeCdc37*—CeCdc37 can in principle react with the dye on three cysteine residues, Cys-212, Cys-311, and Cys-339. Samples of labeled and unlabeled CeCdc37 were analyzed to determine the labeling sites. After protein bands were excised from SDS-PAGE gels, the samples were digested with trypsin. Gel pieces were then treated as described previously (40). Peptides were extracted by washing sequentially with 50 $\mu$l of 0.1% formic acid and 50 $\mu$l of acetonitrile. Collected supernatants were pooled, concentrated to 20 $\mu$l, and filtered through a 0.22-$\mu$m Ultrafree-MC-GV centrifuge filter (Merck Millipore, Tullagreen Carrigtwohill, Ireland). Afterward, they were loaded onto an Acclaim PepMap rapid separation LC $C_{18}$ trap column (Thermo Scientific) at a flow rate of 5 $\mu$l/min and separated on an PepMap rapid separation LC $C_{18}$ column (75 $\mu$m × 150 mm, 2 $\mu$m, 100 Å, Thermo Scientific) at a flow rate of 0.2 $\mu$l/min. A linear gradient from 5 to 35% buffer B (acetonitrile with 0.1% formic acid) eluted the peptides in 60 min to an LTQ Orbitrap XL instrument (Thermo Scientific). Full scans and five dependent MS2 scans (five collision-induced dissociation spectra) were recorded in each cycle. Peptides modified by Alexa Fluor 488-$C_5$-maleimide or iodoacetamide were detected by MaxQuant (41), and the masses of these Alexa Fluor 488-modified peptides were verified to be absent in corresponding MS1 spectra of the unlabeled control sample. Alexa Fluor 488 modifications were detected at positions Cys-311 and Cys-339 in a highly labeled CeCdc37 sample (~85% with two labels and ~15% with one label), but modifications at position 212 were not observed. No iodoacetamide-modified peptide at position Cys-339 was detected in highly labeled CeCdc37, implying that this residue reacts very efficiently with Alexa Fluor 488-$C_5$-maleimide. Cys-311 appears to react slightly less efficiently, and Cys-212 may react only rarely, positioning all attached labels in the C-terminal domain.

*Analytical Ultracentrifugation*—Analytical ultracentrifugation (aUC) experiments were performed in a Beckman ProteomeLab XLA ultracentrifuge equipped with a fluorescence detection system (Aviv Biomedical, Lakewood, NY) and a Ti-50 rotor (Beckman Coulter, Brea, CA) at 20 °C and 42,000 rpm as described previously (35). A 250–500 nM concentration of labeled protein was analyzed by adding a 3–10 $\mu$M concentration of its unlabeled putative binding partner and optionally 4

mM nucleotides. Most measurements were performed in 40 mM HEPES/KOH, pH 7.5, 20 mM KCl, 1 mM DTT, and 5 mM $MgCl_2$. To support the NMR analysis, measurements in 40 mM $KH_2PO_4$/KOH, pH 7.5, also were performed for Cdc37 constructs in complex with Hsp90. Measurements including the kinases were performed in 20 mM Tris/HCl, pH 7.5, 50 mM KCl, 0.5 mM EDTA, 5 mM $MgCl_2$, 1 mM DTT, and 1% (v/v) glycerol. d*c*/d*t* plots were generated with the program SEDVIEW (42, 43), which subtracts scans within a certain range and averages over the differentials. Plots were fit to bi-Gaussian functions to determine the $s_{20,w}$ values and the peak amplitudes.

*Cross-linking with Glutardialdehyde*—Cross-linking experiments with glutardialdehyde (Merck) were performed with fluorescently labeled CeCdc37 and hCdc37. 250 nM labeled hCdc37 and 500 nM labeled CeCdc37 were preincubated alone or in the presence of 2 $\mu$M B-Raf in 20 mM Tris/HCl, pH 7.5, 50 mM KCl, 0.5 mM EDTA, 5 mM $MgCl_2$, 1 mM DTT, and 1% (v/v) glycerol for 10 min at 25 °C. The cross-linking reaction was initiated by the addition of 0.2% (v/v) glutardialdehyde. After an incubation time of 4 min, the reaction was stopped by adding 200 mM Tris/HCl, pH 8.0. Subsequently, samples were separated on SDS-polyacrylamide gradient gels (Serva, Heidelberg, Germany). Fluorescence signals were visualized using a Typhoon 9200 phosphor- and fluorescence imaging system (GE Healthcare) with the settings appropriate for Alexa Fluor 488. To investigate the protein composition, cross-linking was performed with unlabeled proteins at higher concentrations. The presence of both proteins in the respective bands was confirmed by electrospray ionization mass spectrometry on an LTQ Orbitrap XL instrument. Sample preparation and instrument settings were similar to the procedure described above. For cross-link measurements, 2+ ions were rejected. Analysis of the data set was performed with MaxQuant software.

*Fluorescence Spectroscopy with MANT-ADP*—Fluorescence measurements with MANT-ADP (BioLog, Bremen, Germany) were used to detect its binding and release from the kinase B-Raf in the presence of Cdc37 variants as described previously by Polier *et al.* (17). The release of MANT-ADP was recorded using a FluoroMax-3 spectrofluorometer (Horiba Jobin Yvon GmbH, Bernsheim, Germany). The excitation wavelength was set to 290 nm, and emission spectra were recorded from 300 to 550 nm (slit widths, 5 nm) at 10 °C. All measurements were performed in 20 mM Tris/HCl, pH 7.5, 50 mM KCl, 0.5 mM EDTA, 5 mM $MgCl_2$, 1 mM DTT, and 1% (v/v) glycerol. MANT-ADP (120 $\mu$M) was incubated together with a kinase (2 $\mu$M), and optionally Cdc37 variants (3 $\mu$M) were added. Furthermore, MANT-ADP spectra with Cdc37 variants alone were recorded to exclude quenching effects of these constructs in the absence of the kinase. To correct for induced tryptophan fluorescence at the excitation wavelength of 350 nm, appropriate protein spectra were recorded and subtracted from the sample spectra using the Origin 8 software package.

*Anisotropy Measurements*—Experiments were performed with MANT-ADP using the FluoroMax-3 spectrofluorometer. Fluorescence emission was recorded at 446 nm with an excitation at 350 nm. Polarization filters were set to the magic angle, and the instrument-specific G-factor was determined to be to

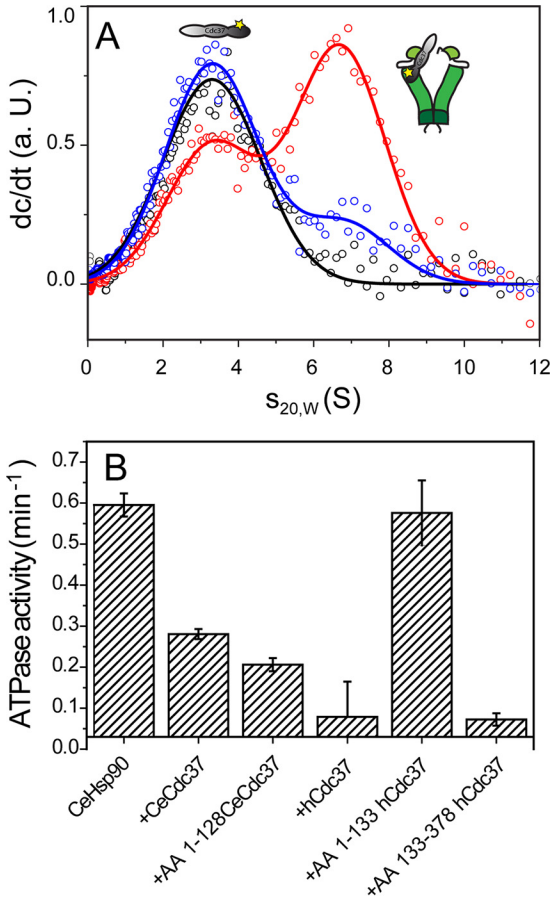


FIGURE 1. **Characterization of CeCdc37(1–128).** *A*, the binding of CeCdc37(1–128) to Hsp90 was tested in an aUC competition experiment. A complex of 500 nM *CeCdc37 (*black*) and 3 $\mu$M CeHsp90 (*red*) was disrupted with an excess of CeCdc37(1–128) (10 $\mu$M) (*blue*). The illustrations symbolize labeled Cdc37 (*gray* with *yellow star*) and Hsp90 (*green*). *B*, the functionality of different Cdc37 fragments was analyzed in an ATPase assay. The activity of 3 $\mu$M CeHsp90 was measured alone and in the presence of a 10 $\mu$M concentration of different Cdc37 constructs at 30 °C. Measurements were performed in 40 mM HEPES/KOH, pH 7.5, 20 mM KCl, 1 mM DTT, and 5 mM $MgCl_2$. *AA*, amino acids; *a.U.*, arbitrary units. *Error bars* represent S.D.

0.6138. The assays were performed at 10 °C in a buffer containing 20 mM Tris/HCl, pH 7.5, 50 mM KCl, 0.5 mM EDTA, 5 mM $MgCl_2$, 1 mM DTT, and 5% (v/v) glycerol. A baseline was recorded for 10 $\mu$M MANT-ADP before adding 3 $\mu$M B-Raf. After obtaining a stable plateau value, a 5 $\mu$M concentration of different Cdc37 constructs was added to compete with MANT-ADP upon B-Raf binding. Data analysis was carried out applying a single exponential function.

*NMR Spectroscopy*—NMR spectra were recorded on Bruker AV900, AV750, and AV600 spectrometers equipped with a TCI cryoprobe or room temperature (AV750) probe heads (Bruker) at 25 °C unless mentioned otherwise. Two-dimensional $^{1}H$-$^{15}N$ water-flip-back heteronuclear single quantum coherence correlation experiments were measured for two CeCdc37 fragments, CeCdc37(1–128) and CeCdc37(36–128). The proteins were isotopically labeled with $^{13}C$ and/or $^{15}N$ by growing cells in standard M9 medium containing 2 g/liter [$^{13}C$]glucose and/or 1 g/liter [$^{15}N$]ammonium chloride. The labeled proteins were purified as described previously and dialyzed against storage buffer containing 40 mM $KH_2PO_4$/KOH, pH 7.5, with 8% $D_2O$ (v/v) added. In the case of CeCdc37(36–128), the $His_6$ tag

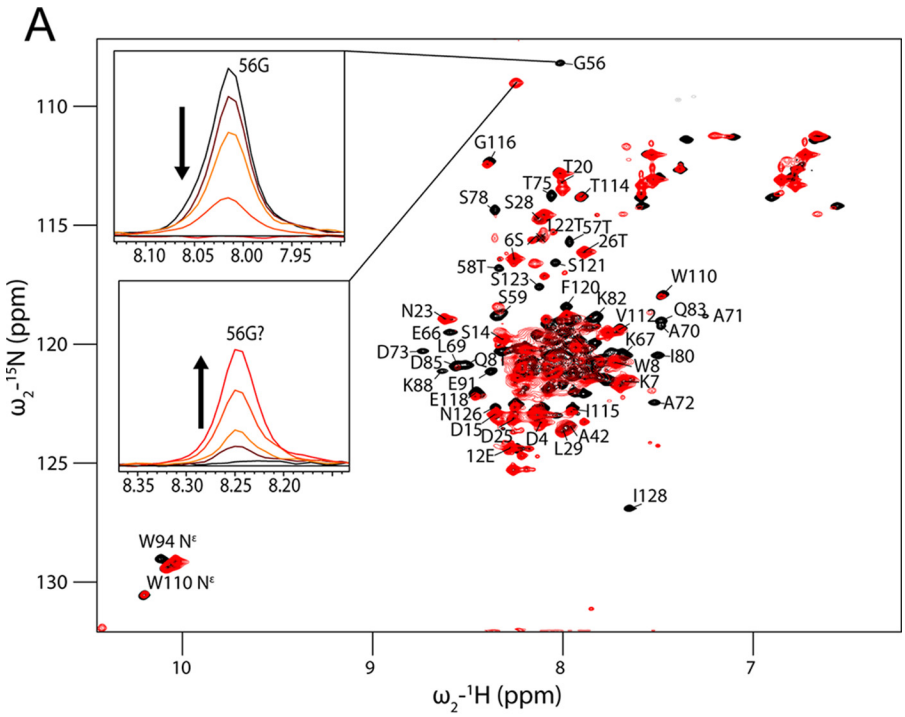


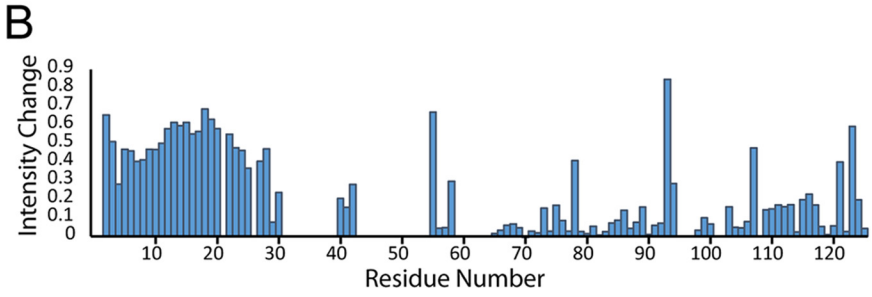


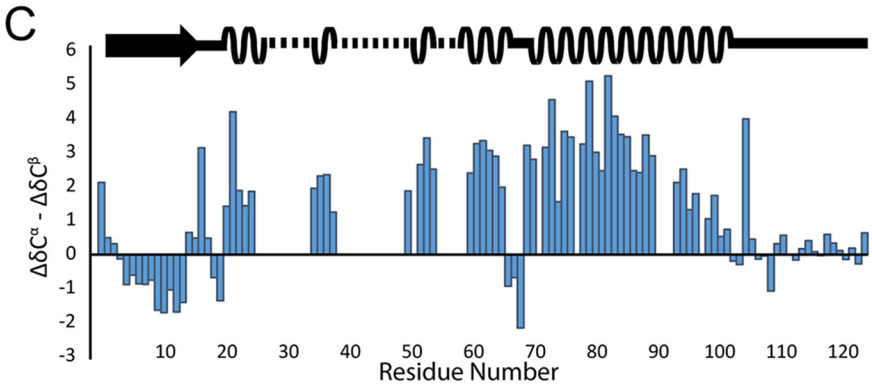


D

```
CeCdc37         MPIDYSKWKDIEVSDDEDDTHPNIDTPSLFRWRHQARLERMAEKKMEQEKIDKEKGTTSK 60
hCdc37          -MVDYSVWDHIEVSDDEDETHPNIDTASLFRWRHQARVERMEQFQKEKEELDRGCRECKR 59
                  :*** *..********:*******.**********:*** : : *:*::*:     .:

CeCdc37         KMEELEKKLAAADVTD--KSD---IQKQIDEVKAQEEANKKKEAELEEKERLEPWNVDTI 115
hCdc37          KVAECQRKLKELEVAEGGKAELERLQAEAQQLRKEERSWEQKLEEMRKKEKSMPWNVDIL 119
                *: * ::**   :*::  *::   :* : :::: :*.:  .:*  *:.:**:  ******:

CeCdc37         GHEAFSTSRINKI- 128
hCdc37          SKDGFSKSMVNTKP 133
                .:::.**.* :*.
```

was removed with thrombin followed by an additional purification step on a nickel-nitrilotriacetic acid column. Unlabeled middle domain of CeHsp90 (CeHsp90M) was added to a 1.5-fold excess to each construct of CeCdc37. Spectra were processed with NMRPipe (44) and analyzed using CcpNMR Analysis (45). Assignments were obtained using standard triple resonance water-flip-back backbone assignment experiments: HNCA, HNCaCb, CbCa(co)NH, HNCO, HN(ca)CO, (H)CC(co)NH total correlation spectroscopy, and three-dimensional $^{15}$N-edited NOESY (46).

## Results

*The N Terminus of CeCdc37 Is Sufficient to Interact with CeHsp90*—Differences between hCdc37 and CeCdc37 regarding their interaction sites with Hsp90 were observed in previous studies (32). The nematode cochaperone binds with parts of the N terminus to the Hsp90M, whereas for hCdc37(138–C) (where C represents the C terminus), the N-terminal domain of Hsp90 is the prominent binding site. So far, structural information is only available for the human cochaperone in complex with yeast Hsp90 (33). Thus, we wanted to obtain a more detailed view on the interaction in the nematode complex. We expressed and purified the N-terminal part of CeCdc37 containing amino acids 1–128 and performed a binding analysis of this fragment using an established aUC competition experiment with labeled full-length CeCdc37 (*CeCdc37). A complex of *CeCdc37·Hsp90 was formed, and the ability of the N-terminal fragment to disrupt the complex was investigated by adding an excess amount of CeCdc37(1–128) (Fig. 1*A*). This CeCdc37 fragment could indeed compete against the full-length CeCdc37, showing its ability to interact with Hsp90 in a similar manner as full-length CeCdc37. We further tested the functional importance of CeCdc37(1–128) in an ATPase assay as CeCdc37 was found to inhibit the ATP turnover of Hsp90 (Fig. 1*B*). The short fragment was able to decrease the ATPase activity of CeHsp90 in a similar manner as WT CeCdc37. These results imply that the CeCdc37 fragment harboring the first 128 amino acids contains the most important parts to bind and inhibit Hsp90. Contrarily, the corresponding fragment of human Cdc37 (hCdc37(1–133)) was not capable of influencing the ATP turnover of CeHsp90. Instead, here the C-terminal part (hCdc37(133–C)) contains an inhibiting activity similar to full-length hCdc37 (Fig. 1*B*).

*The CeCdc37/Hsp90M Interaction Depends on a Trp and an Arg Residue*—To identify residues involved in the interaction between CeCdc37 and CeHsp90, we performed NMR titrations (Fig. 2, *A* and *B*). To this end, the CeCdc37(1–128) fragment was isotopically labeled with $^{15}$N and $^{1}$H, and $^{15}$N heteronuclear single quantum coherence NMR spectra were recorded. The protein was stable in the temperature range between 5 and 37 °C with only small differential chemical shift changes observed for some NMR signals with increasing temperature (data not shown).

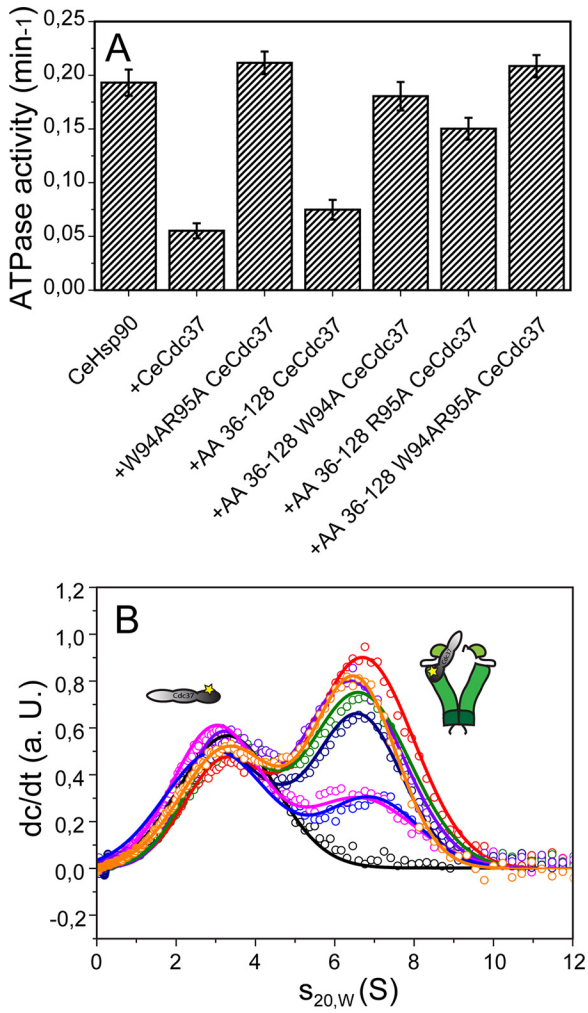


FIGURE 3. **Trp-94 and Arg-95 of CeCdc37 are crucial for binding to Hsp90M.** *A*, the functionality of CeCdc37(36–128) was tested in an ATPase assay measured at 25 °C. The activity of 3 $\mu$M CeHsp90 was analyzed in the presence of 10 $\mu$M CeCdc37, W94A/R95A CeCdc37, CeCdc37(36–128), W94A CeCdc37(36–128), R95A CeCdc37(36–128), and W94A/R95A CeCdc37(36–128). *B*, an aUC competition experiment was performed with 500 nM *CeCdc37 (*black*) in complex with 3 $\mu$M CeHsp90 (*red*), which was challenged by either 10 $\mu$M unlabeled CeCdc37 (*blue*), W94A/R95A CeCdc37 (*orange*), CeCdc37(36–128) (*magenta*), W94A CeCdc37(36–128) (*green*), R95A CeCdc37(36–128) (*marine blue*), or W94A/R95A CeCdc37(36–128) (*purple*). The illustrations symbolize labeled Cdc37 (*gray* with a *yellow star*) and Hsp90 (*green*). *AA*, amino acids; *a.U.*, arbitrary units. *Error bars* represent S.D.

Backbone chemical shift assignments were obtained for 94 of 124 non-proline residues. Several regions could not be assigned due to extensive overlap present in the spectra. For several residues in the C-terminal region, a second minor signal is observed, potentially resulting from proline isomerization or a

FIGURE 2. **NMR titration of CeCdc37(1–128) with CeHsp90M.** *A*, $^{1}$H-$^{15}$N heteronuclear single quantum coherence spectra of CeCdc37(1–128) free (*black*) and bound with CeHsp90M (*red*). *Insets* are one-dimensional traces of individual peaks throughout titration of Gly-56 bound and free of CeCdc37(1–128) with CeHsp90M at 0 (*black*), 0.1 (*dark orange*), 0.2 (*orange*), 0.5 (*orange-red*), and 1 (*red*) molar eq. *B*, relative intensity of each peak comparing CeHsp90M bound *versus* free CeCdc37(1–128). *C*, secondary chemical shift differences of $^{13}C^{\alpha}$ and $^{13}C^{\beta}$ compared with random coil shifts. Positive and negative values indicate $\alpha$-helical and $\beta$-strand conformations, respectively; values close to 0 are found for random coil conformation. The *dashed line* denotes regions without backbone assignments. *D*, sequence alignment of CeCdc37(1–128) and hCdc37(1–133) using the ClustalW2 software. The *stars* indicate conserved amino acids, *two dots* symbolize groups of strongly similar properties, and *one dot* represents groups of weakly similar properties. Additionally, a sequence prediction was performed using Jpred 3. Helical motifs are highlighted in *orange*, and extended regions are in *blue*. The *red circle* highlights the two amino acids relevant for the interaction with CeHsp90M.

minor residual state in the C terminus. Based on the secondary chemical shift differences of the $^{13}C^{\alpha}$ and $^{13}C^{\beta}$ resonances, the majority of CeCdc37(1–128) adopts an $\alpha$-helical conformation (Fig. 2*C*). In contrast, residues 9–25 appear to adopt an extended conformation, whereas the C-terminal residues 105–128 adopt a random coil conformation. These observations are consistent with secondary structure predictions using the program Jpred, which predicted this fragment of CeCdc37 as mostly $\alpha$-helical (Fig. 2*D*).

To map the binding interface with CeHsp90M, spectra were recorded for $^{15}N$-labeled CeCdc37(1–128) alone and in the presence of CeHsp90M at 25 °C. Upon addition of CeHsp90M, many of the amide signals of CeCdc37(1–128) disappear or experience severe line broadening. Moreover, a number of new signals appear at different positions in the spectrum. Unfortunately, due to the poor spectra quality in the bound state and the observed instability of CeHsp90M in NMR conditions, most of the new NMR signals could not been assigned (Fig. 2*A*). Interestingly, the regions from 1–30 appear to be largely unaffected by CeHsp90M binding, whereas residues 44–128 show a significant reduction in signal intensities or chemical shift changes. When comparing the two spectra, it is apparent that the chemical shifts of a Trp side chain and an Arg side chain are influenced by the addition of CeHsp90M. Thus, it can be expected that these two amino acids of CeCdc37 are located in a region that is influenced by the binding event. We were able to assign the tryptophan to Trp-94 but were unable to unambiguously assign the corresponding arginine side chain.

Our NMR results suggest that the N-terminal region in Cdc37 is not involved in interactions with Hsp90. To confirm this, we generated a shorter construct comprising only amino acids 36–128 lacking the $His_6$ tag. Using our aUC setup, we find that this fragment is sufficient to bind to Hsp90 and is also able to inhibit the activity of Hsp90 in ATPase assays (Fig. 3, *A* and *B*). The fact that most NMR signals in the shorter construct fully superimpose with those observed for CeCdc37(1–128) further confirms that the N-terminal amino acids do not (strongly) interact or modulate the structure of the core domain of Cdc37.

*Mutation of Trp-94 and Arg-95 Disrupts Complex Formation*—We wanted to identify potential residues that are critical for the interaction between CeCdc37 and CeHsp90M. Our NMR experiments brought our attention to Trp-94, which is next to Arg-95, making them well positioned to be involved in the binding event (Fig. 2*D*). To resolve whether these two residues play a role during complex formation, both of them were mutated to Ala residues in CeCdc37(36–128). Indeed, W94A/R95A CeCdc37(36–128) could not inhibit the ATP turnover of CeHsp90 nor could it compete with WT CeCdc37 for CeHsp90 binding in the aUC (Fig. 3, *A* and *B*). To distinguish whether both amino acids are necessary, single point mutants were also generated. We find that already W94A CeCdc37(36–128) is severely compromised in its interaction with Hsp90 and also in its inhibitory function toward the ATPase activity of Hsp90 (Fig. 3, *A* and *B*). Mutating only Arg-95 to alanine also results in a decreased ability to inhibit the ATPase activity of Hsp90 and in a diminished complex formation with the chaperone in the aUC (Fig. 3, *A* and *B*). Next, we exchanged these two residues in WT CeCdc37 (W94A/R95A CeCdc37) and analyzed its functionality and binding ability toward CeHsp90 (Fig. 3, *A* and *B*). Similar to the engineered point mutants in the N-terminal frag-

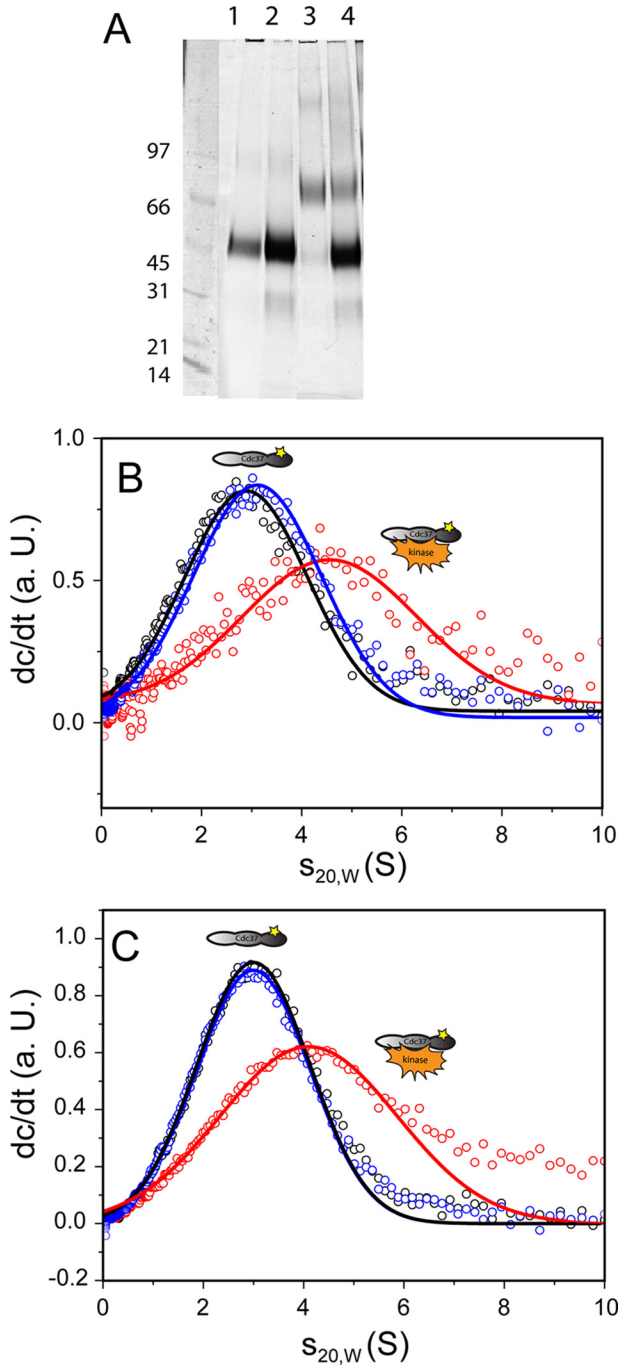


FIGURE 4. **Cdc37·B-Raf complex formation is conserved.** *A*, a cross-linking experiment of labeled Cdc37 with B-Raf was performed using glutardialdehyde. 250 nM *hCdc37 is shown in *lane 1* and as a cross-link with 2 $\mu$M B-Raf in *lane 3*. The same experiment but using 500 nM *C. elegans* cochaperone is shown in *lane 2* and in complex with B-Raf in *lane 4*. *B*, an aUC experiment was performed with 500 nM labeled *hCdc37 (*black*) in complex with 3 $\mu$M B-Raf (*red*). This complex formation was disrupted by adding 4 mM ATP (*blue*). In *C*, a similar aUC experiment was performed, but instead of human Cdc37 the labeled *C. elegans* protein (500 nM) was used. All measurements were carried out in 20 mM Tris/HCl, pH 7.5, 50 mM KCl, 0.5 mM EDTA, 5 mM $MgCl_2$, 1 mM DTT, and 1% (v/v) glycerol. The illustrations symbolize labeled Cdc37 (*gray* with a *yellow star*) and the kinase (*orange*). *a.U.*, arbitrary units.

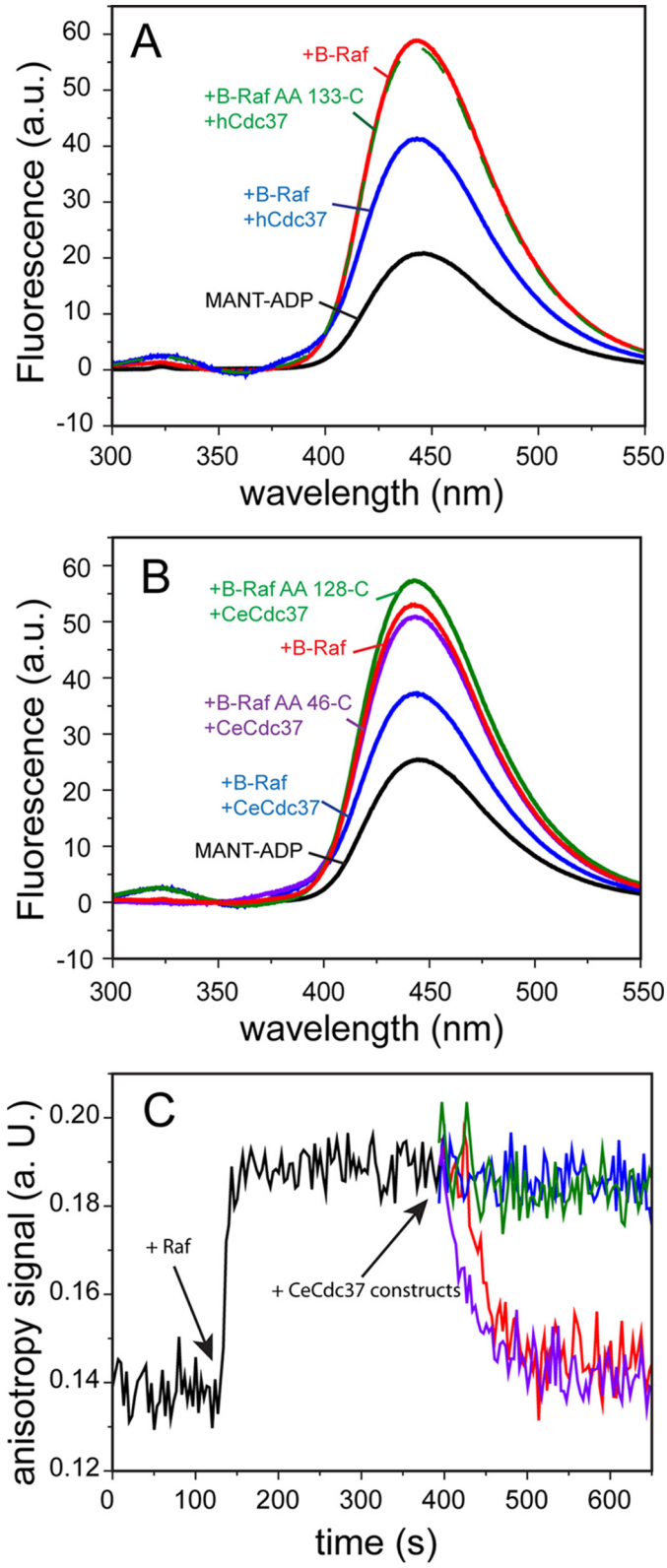


FIGURE 5. **The very N terminus of Cdc37 weakens binding of ADP to B-Raf.** *A* and *B*, a fluorescence-based assay with 120 $\mu$M MANT-ADP (*black*) was performed to analyze the binding ability of 2 $\mu$M B-Raf kinase (*red*). The excitation wavelength was set to 290 nm. *A*, the binding of the nucleotide was challenged by addition of 3 $\mu$M hCdc37 (*blue*) or 3 $\mu$M hCdc37(133–C) (*green*). *B*, 3 $\mu$M CeCdc37 (*blue*), CeCdc37(128–C) (*green*), or CeCdc37(46–C) (purple) were added to the preformed MANT-ADP/B-Raf mixture. *C*, in addition to the fluorescence-based MANT-ADP assay, an anisotropy assay was performed with an excitation wavelength of 350 nm and an emission of 446 nm. After measuring a baseline of 10 $\mu$M MANT-ADP alone, 3 $\mu$M B-Raf was added to the assay, leading to an increase of the signal (marked with an *arrow*). After reaching a plateau value, a 5 $\mu$M concentration of different CeCdc37 constructs was added: CeCdc37 (*red*), CeCdc37(1–284) (*blue*), CeCdc37(15–C) (*purple*), and CeCdc37(26–C) (*green*). All measurements were performed at 10 °C in 20 mM Tris/HCl, pH 7.5, 50 mM KCl, 0.5 mM EDTA, 5 mM $MgCl_2$, 1 mM DTT, and 1% (v/v) glycerol (*A* and *B*) or 5% (v/v) glycerol (*C*). *AA*, amino acids; *a.U.*, arbitrary units.

ment of CeCdc37, the mutated WT protein could not bind to CeHsp90 nor could it inhibit its ATP turnover. These results show that the tryptophan at position 94 and the arginine at position 95 are involved in the binding to Hsp90 and are important to inhibit its ATP turnover in the nematode Hsp90·Cdc37 complex.

*B-Raf Interacts with Nematode Cdc37 Similarly to Human Cdc37*—Given the considerable differences between the two Cdc37 homologs during Hsp90 binding, we next aimed at studying the kinase interaction in the human and nematode Cdc37 proteins. To this end, we utilized the solubilized kinase domain of the human B-Raf kinase, which recently was shown to form a complex with human Cdc37 by Polier *et al.* (17). We performed a cross-linking experiment to test whether B-Raf interacts with Cdc37 of both species (Fig. 4*A*). In this experiment, the cochaperone was fluorescently labeled (marked with an asterisk). *CeCdc37 and *hCdc37 by themselves produced no dimeric or higher oligomeric cross-linking products after incubation with glutardialdehyde. Interestingly, in the presence of B-Raf kinase, the *hCdc37 band is strongly diminished, and a specific band at higher molecular weight appears (Fig. 4*A*). Using mass spectrometry, this band was found to contain both proteins, Cdc37 and the B-Raf kinase. Based on the 70-kDa size of this cross-linking product, it is to be assumed that one *hCdc37 is trapped in complex with one B-Raf molecule. The same behavior can be observed for *CeCdc37, implying that the stabilized kinase domain of B-Raf may also directly interact with CeCdc37.

To confirm the binding of B-Raf to CeCdc37, we performed analytical ultracentrifugation with fluorescently labeled Cdc37 (Fig. 4, *B* and *C*). Both *Cdc37 proteins sediment with an $s_{20,w}$ value of 2.9 ± 0.2 S. In complex with B-Raf, both labeled *Cdc37 proteins sediment with a higher sedimentation coefficient (*CeCdc37, 4.1 ± 0.4 S; *hCdc37, 4.4 ± 0.3S), confirming that despite the differences in Hsp90 interaction both Cdc37s are capable of interacting with B-Raf in a similar manner. Polier *et al.* (17) have further shown that ATP can disrupt the hCdc37·kinase complex. To see whether this effect is also observable for the nematode cochaperone, we added ATP to the preformed *CeCdc37·B-Raf complex (Fig. 4, *B* and *C*). Indeed, the nucleotide disrupted the interaction of B-Raf with human and *C. elegans* Cdc37, leading to a dissociation of the protein complex and sedimentation of Cdc37 as an uncomplexed monomeric protein.

*The N-terminal Part of CeCdc37 Diminishes Nucleotide Binding to B-Raf*—The N terminus of human Cdc37 has been shown to release a bound nucleotide from the kinase domain of B-Raf (17). We thus tested whether CeCdc37 is also able to release the nucleotide from the kinase via its N-terminal domain. A fluorescence-based assay with MANT-ADP established by Polier *et al.* (17) was used to analyze nematode Cdc37

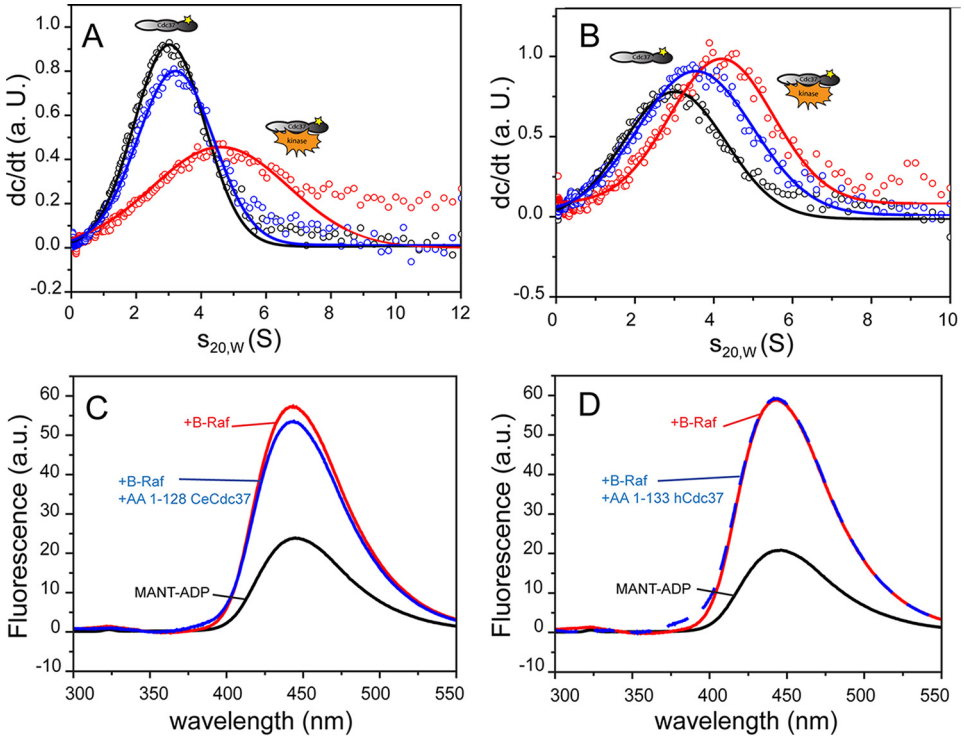


FIGURE 6. **The C-terminal part of Cdc37 is required for B-Raf binding.** *A*, an aUC experiment was performed with 250 nM labeled *CeCdc37 (*black*) in complex with 3 $\mu$M B-Raf (*red*). This complex was challenged by adding 10 $\mu$M CeCdc37(128–C) (*blue*). *B*, the same experiment as in *A* was carried out, but this time labeled *hCdc37 was used, and the complex was challenged by adding 10 $\mu$M hCdc37(133–C). The illustrations symbolize labeled Cdc37 (*gray* with a *yellow star*) and Hsp90 (*green*). *C*, the binding ability of 2 $\mu$M B-Raf (*red*) toward 120 $\mu$M MANT-ADP (*black*) was analyzed in a fluorescence-based assay. The excitation wavelength was set to 290 nm. The binding of the nucleotide was challenged by adding 3 $\mu$M CeCdc37(1–128) (*blue*). *D*, the same experiment as in *C* was performed, but the B-Raf·MANT-ADP complex was challenged with 3 $\mu$M hCdc37(1–133). 20 mM Tris/HCl, pH 7.5, 50 mM KCl, 0.5 mM EDTA, 5 mM $MgCl_2$, 1 mM DTT, and 1% (v/v) glycerol was the buffer used for all measurements. *AA*, amino acids; *a.U.*, *a.u.*, arbitrary units.

fragments in this respect (Fig. 5, *A* and *B*). We could detect a competition against MANT-ADP with full-length nematode Cdc37 similar to the human protein. When we deleted the first 128 amino acids of CeCdc37, this fragment was no longer able to compete off the nucleotide from B-Raf (Fig. 5*B*), implying that this mechanism could be similar to the one reported for the hCdc37 (Fig. 5*A*). Even when deleting only the first 46 amino acids of CeCdc37, MANT-ADP still remains bound to the kinase (Fig. 5*B*).

We next aimed at analyzing the reaction of nucleotide displacement kinetically. To this end, we used an anisotropy setup of the same assay (Fig. 5*C*). In this experiment, an increase in anisotropy signal can be observed upon binding of B-Raf to MANT-ADP. This increase is fast and happens during the mixing period. Addition of CeCdc37 results in a decrease of the anisotropy signal consistent with the release of nucleotide. A half-time value of $t_{1/2} = 37 \pm 3$ s can be envisioned from this reaction, implying that the displacement of the nucleotide might be rather slow. We then tested whether different CeCdc37 constructs can result in a similar reaction. A deletion of only 25 amino acids from the N terminus of CeCdc37 does not lead to a drop in anisotropy values similar to a fragment lacking the entire N-terminal domain (Fig. 5*C*). A fragment lacking only the first 14 amino acids instead could still displace the nucleotide, suggesting that important residues for this reaction reside between amino acids 15 and 25 of CeCdc37.

*B-Raf Binding Is Mediated by the C-terminal Domain of Cdc37*—As B-Raf binds to CeCdc37 and hCdc37, we wondered which part of the cochaperone is additionally required to form the binding site. Using various truncation mutants, we tested whether specific deletion constructs of Cdc37 are capable to compete for B-Raf binding with *CeCdc37 in aUC experiments (Fig. 6, *A* and *B*). Surprisingly, a deletion of the N-terminal part of the cochaperone (Δ128 CeCdc37) was still very efficient in competing against complex formation, implying that upon deletion of the N-terminal amino acids the binding affinity is not lost despite the inability to displace the nucleotide (Fig. 6*A*). The same was evident in experiments with human Cdc37 fragments (Fig. 6*B*). Performing the same assay with N-terminal Cdc37 fragments (CeCdc37(1–128) and hCdc37(1–133)) resulted in no detectable competition against full-length Cdc37 (data not shown), confirming that C-terminal parts have to contribute affinity to this binding reaction to enable the N-terminal part of CeCdc37 to exchange the nucleotide.

Hence, we examined further truncation mutants of the C-terminal region of CeCdc37 (CeCdc37(128–284) and CeCdc37(284–C)). With these fragments, we could not observe competition against the full-length cochaperone for B-Raf binding in aUC experiments (data not shown). This highlights that the interaction with B-Raf is mediated mostly by the C-terminal part of Cdc37 with contributions of the middle domain. We additionally tested whether the truncation mutants lacking the C-terminal domain are able to prevent

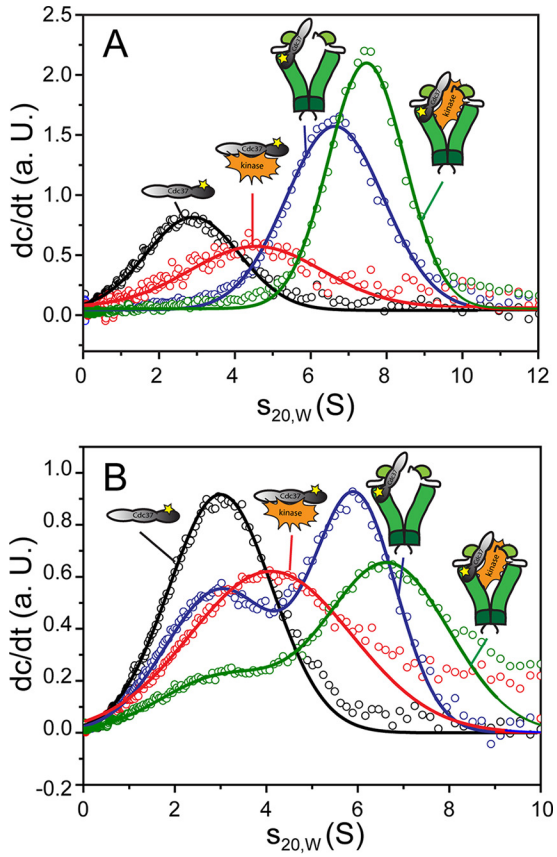


FIGURE 7. **Formation of the ternary complex of Hsp90·Cdc37·B-Raf.** *A*, the formation of a ternary complex of Hsp90, Cdc37, and B-Raf was analyzed in the aUC. 250 nM *hCdc37 (*black*) was measured in complex with 3 $\mu$M hHsp90 (*blue*), 3 $\mu$M B-Raf (*red*) and hHsp90·B-Raf (*green*). *B*, the same aUC experiment as in *A* was performed but this time with 250 nM *CeCdc37 (*black*) in complex with 3 $\mu$M CeHsp90 (*blue*), 3 $\mu$M B-Raf (*red*), and CeHsp90·B-Raf (*green*). All measurements were performed in 20 mM Tris/HCl, pH 7.5, 50 mM KCl, 0.5 mM EDTA, 5 mM $MgCl_2$, 1 mM DTT, and 1% (v/v) glycerol. The illustrations symbolize labeled Cdc37 (*gray* with a *yellow star*), Hsp90 (*green*), and the kinase (*orange*). *a.U.*, arbitrary units.

binding of MANT-ADP (Fig. 6, *C* and *D*). This indeed was not the case, confirming that the C terminus of Cdc37 is required for binding of Cdc37 to B-Raf, whereas the N terminus of the cochaperone is required for nucleotide release.

*Ternary Complexes with CeHsp90 Are Formed with B-Raf*—Having defined the interaction between Cdc37 and B-Raf, we wanted to see whether also a ternary complex with Hsp90 can be formed. We used the aUC setup with labeled Cdc37 constructs and added the organism-specific Hsp90 alone and in combination with B-Raf (Fig. 7, *A* and *B*). *CeCdc37 and *hCdc37 interact with Hsp90 alone and with B-Raf. Importantly, in the presence of B-Raf, a shift of the *hCdc37·hHsp90 complex peak from 6.3 to 7.9 S can be observed. Likewise, a shift from 6.1 to 7.0 S can be observed for *CeCdc37·CeHsp90 under the same conditions. Although all *hCdc37 had formed complexes at 7.9 S, residual free *CeCdc37 is present at the same protein concentrations. These results show a slightly weaker interaction between B-Raf and CeCdc37·CeHsp90 compared with hCdc37·hHsp90. Furthermore, they confirm that the ternary complex can be formed in both systems, pointing to a highly conserved mechanism in respect to kinase binding in these two organisms.

*The Protein Kinase Erk2 Shares Specific Features of the Cdc37/B-Raf Interaction*—We finally wanted to know whether other kinases are able to interact with CeCdc37 in a manner similar to B-Raf (47). To this end, we utilized the labeled *CeCdc37 in analytical ultracentrifugation experiments and supplemented the mitogen-activated protein kinase Erk2 (Fig. 8*A*). Similar to B-Raf, we could observe a peak shift to higher $s_{20,w}$ values (complex peak at 4.8 ± 0.4 S), showing the potential of *CeCdc37 to interact also with Erk2. We tested the specificity of these interactions by competition experiments. After addition of hCdc37, the complex of *CeCdc37 and Erk2 is reduced but still apparent, indicating that the efficiency of complex formation is reduced compared with the B-Raf kinase (Fig. 8*A*). We also included ATP in these sedimentation experiments. Indeed, the ability of Erk2 to form complexes with *CeCdc37 is markedly reduced in the presence of the nucleotide, showing that this feature of the interaction is conserved between B-Raf and Erk2 (Fig. 8*A*). We further wanted to know whether N- and C-terminal fragments of hCdc37 can compete against the *CeCdc37·Erk2 complexes (Fig. 8*B*). Here, in contrast to previous experiments with B-Raf, we do not observe significant competition with either deletion fragment, suggesting that for this kinase the interaction requires both the N-terminal and C-terminal parts of hCdc37. Despite these differences in the interaction mode with Cdc37, we could still observe a ternary Hsp90·Cdc37·Erk2 complex at 7.3 ± 0.3 S compared with the binary Cdc37·Hsp90 complex, which sediments at 6.8 ± 0.3 S (Fig. 8*C*). These observations point to a chaperone assembly that is conserved also for Erk2 but apparently with distinct features that appear to depend on specific characteristics of the kinase.

## Discussion

In this study, we characterized the interaction of the molecular chaperone Hsp90 and its cofactor Cdc37 with kinases. Previous experiments suggested a second binding site between the two proteins including the N-terminal part of CeCdc37 and the middle domain of Hsp90 (32). So far, only structural information of the N-terminal domain of yeast Hsp90 with the C-terminal domain of hCdc37 is available by crystallography and NMR spectroscopy (33, 48).

By analyzing the structure of the *C. elegans* proteins by NMR spectroscopy, we could identify that Trp-94 and Arg-95 in the N-terminal domain of nematode Cdc37 are involved in the secondary binding site (Fig. 9). Mutation of these sites to alanine results in loss of the interaction. In the human protein, only the Trp residue is conserved, whereas the arginine and several other amino acids in this region are distinct. Apparently, this binding site becomes undetectable if isolated from the rest of the binding interfaces in the human complex due to these amino acid changes.

In regard to the interaction between Cdc37 and protein kinases, the conserved nature between human and nematode systems is very obvious. Formation of the kinase·Cdc37 complex is readily visible in analytical ultracentrifugation experiments, cross-linking experiments, and fluorescence assays. The competition between Cdc37 binding and nucleotide binding to the kinase is dependent on the presence of the N-terminal

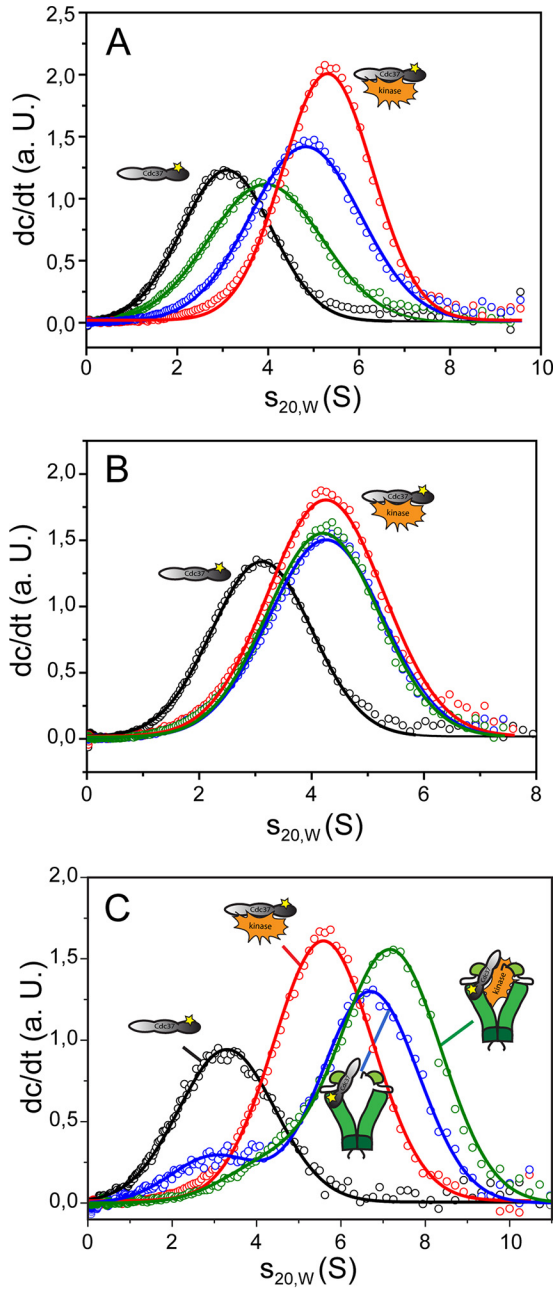


FIGURE 8. **The MAP kinase Erk2 also forms ternary complexes with Hsp90·Cdc37.** *A*, the binding ability of Erk2 was analyzed in the aUC using 250 nM *CeCdc37 (*black*). The complex with 4 $\mu$M Erk2 is depicted in *red*, a competition experiment with 10 $\mu$M hCdc37 is in *blue*, and that with 4 mM ATP is in *green*. *B*, the complex of 250 nM *CeCdc37 (*black*) and 3 $\mu$M Erk2 (*red*) was also challenged with 10 $\mu$M hCdc37(1–133) (*blue*) and 10 $\mu$M hCdc37(133–C) (*green*) in the aUC. *C*, 250 nM *CeCdc37 (*black*) was analyzed in complex with 3 $\mu$M CeHsp90 (*blue*) and 5 $\mu$M Erk2 (*red*) and in a ternary complex with CeHsp90 (3 $\mu$M) and Erk2 (5 $\mu$M) (*green*) using aUC. All measurements were performed in 20 mM Tris/HCl, pH 7.5, 50 mM KCl, 0.5 mM EDTA, 5 mM $MgCl_2$, 1 mM DTT, and 1% (v/v) glycerol. The illustrations symbolize labeled Cdc37 (*gray* with a *yellow star*), Hsp90 (*green*), and the kinase (*orange*). *a.U.*, arbitrary units.

amino acids of Cdc37. Here apparently important amino acids reside in a highly conserved stretch between amino acids 15 and 25 and only in the presence of this part can release of the nucleotide from the kinase be observed. Surprisingly, we find that the interaction between B-Raf kinase and both Cdc37s requires the C-terminal domain of Cdc37. This allows differentiation

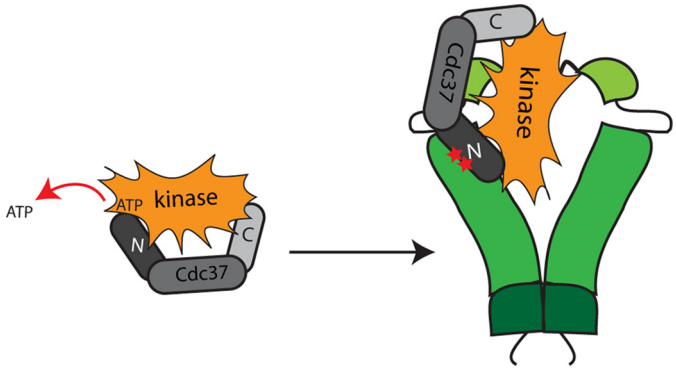


FIGURE 9. **Model of the ternary complex of kinase, Cdc37, and Hsp90.** The model is based on the interaction sites defined for the human protein by Polier *et al.* (17) and for the nematode protein defined in this study. The interaction of kinase with Hsp90 is hypothetical as there is only limited information whether one domain participates or both subunits of Hsp90 are involved. Hsp90 is depicted in *green*, the kinase is in *orange*, and Cdc37 is in *gray*. The *red stars* mark Trp-94 and Arg-95, which are relevant for the interaction of Cdc37 with the middle domain of Hsp90.

between a functional N-terminal part of Cdc37 harboring the nucleotide exchange activity for kinases and a C-terminal part relevant for providing the binding affinity. Furthermore, there appear to be significant variations in the interaction between Cdc37 and different kinase clients. Although a similar relationship between Cdc37 binding and nucleotide binding can be observed for the kinase Erk2, the complex formation between Cdc37 and this kinase appears to be weaker compared with B-Raf. Interestingly, a cooperative contribution of the N- and C-terminal regions of Cdc37 could be observed for this kinase as deletion of each region leads to a loss of interaction with the cochaperone. Even though BLAST searches show that the kinase domains of Erk2 and B-Raf share only an identity of 24%, the overall structure of these domains is very similar (kinase domain of Erk2, Protein Data Bank in Europe code 3sa0; kinase domain of B-Raf, Protein Data Bank in Europe code 3omv). A reason for the different binding behavior toward Cdc37 could also be the extended C-terminal tail of the Erk2 full-length protein or the fact that the B-Raf studied herein contained solely the solubilized kinase domain of the protein. These results imply that the parameters of kinase·Cdc37 complex formation could be features that are highly kinase-dependent.

We also gained information on the binding sites used in ternary complexes. These results suggest a model where four contacts are involved, two between Cdc37 and Hsp90 and two between Cdc37 and the protein kinase (Fig. 9). The C-terminal part of Cdc37 interacts only with the kinase, whereas the N-terminal domain is bound to Hsp90 but can simultaneously interfere with the nucleotide binding pocket of the kinase. It still remains an open question how a client is attached to Hsp90, in particular as binding sites in the N-terminal, middle, and C-terminal domains of Hsp90 have been shown to be important for client interactions (9, 25, 49). Given the ample number of binding sites between Cdc37 and kinase and between Cdc37 and Hsp90, it certainly argues for a closely assembled and regulated protein complex participating in the maturation of protein kinases.

*Author Contributions*—J. M. E., M. J. S., and K. R. conceived and designed the experiments. L. F. and M. S. performed and analyzed the NMR experiment. M. A. D. performed the mass experiment. J. M. E., M. J. S., and K. R. performed and analyzed all other experiments. J. M. S., K. R., L. F., and M. S. wrote the paper.

*Acknowledgments—We thank Chris Prodromou for the B-Raf-containing expression plasmid and Adrian Drazic for critically reading the manuscript.*

## References


1. Rubin, G. M., Yandell, M. D., Wortman, J. R., Gabor Miklos, G. L., Nelson, C. R., Hariharan, I. K., Fortini, M. E., Li, P. W., Apweiler, R., Fleischmann, W., Cherry, J. M., Henikoff, S., Skupski, M. P., Misra, S., Ashburner, M., Birney, E., Boguski, M. S., Brody, T., Brokstein, P., Celniker, S. E., Chervitz, S. A., Coates, D., Cravchik, A., Gabrielian, A., Galle, R. F., Gelbart, W. M., George, R. A., Goldstein, L. S., Gong, F., Guan, P., Harris, N. L., Hay, B. A., Hoskins, R. A., Li, J., Li, Z., Hynes, R. O., Jones, S. J., Kuehl, P. M., Lemaitre, B., Littleton, J. T., Morrison, D. K., Mungall, C., O'Farrell, P. H., Pickeral, O. K., Shue, C., Vosshall, L. B., Zhang, J., Zhao, Q., Zheng, X. H., and Lewis, S. (2000) Comparative genomics of the eukaryotes. *Science* **287,** 2204–2215
2. Caplan, A. J., Mandal, A. K., and Theodoraki, M. A. (2007) Molecular chaperones and protein kinase quality control. *Trends Cell Biology* **17,** 87–92
3. Hanks, S. K., Quinn, A. M., and Hunter, T. (1988) The protein kinase family: conserved features and deduced phylogeny of the catalytic domains. *Science* **241,** 42–52
4. Hubbard, S. R., and Till, J. H. (2000) Protein tyrosine kinase structure and function. *Annu. Rev. Biochem.* **69,** 373–398
5. Pearl, L. H., and Prodromou, C. (2006) Structure and mechanism of the Hsp90 molecular chaperone machinery. *Annu. Rev. Biochem.* **75,** 271–294
6. Taipale, M., Krykbaeva, I., Koeva, M., Kayatekin, C., Westover, K. D., Karras, G. I., and Lindquist, S. (2012) Quantitative analysis of HSP90-client interactions reveals principles of substrate recognition. *Cell* **150,** 987–1001
7. Picard, D. (2002) Heat-shock protein 90, a chaperone for folding and regulation. *Cell. Mol. Life Sci.* **59,** 1640–1648
8. Echeverría, P. C., Bernthaler, A., Dupuis, P., Mayer, B., and Picard, D. (2011) An interaction network predicted from public data as a discovery tool: application to the Hsp90 molecular chaperone machine. *PLoS One* **6,** e26044
9. Vaughan, C. K., Gohlke, U., Sobott, F., Good, V. M., Ali, M. M., Prodromou, C., Robinson, C. V., Saibil, H. R., and Pearl, L. H. (2006) Structure of an Hsp90-Cdc37-Cdk4 complex. *Mol. Cell* **23,** 697–707
10. Vaughan, C. K., Mollapour, M., Smith, J. R., Truman, A., Hu, B., Good, V. M., Panaretou, B., Neckers, L., Clarke, P. A., Workman, P., Piper, P. W., Prodromou, C., and Pearl, L. H. (2008) Hsp90-dependent activation of protein kinases is regulated by chaperone-targeted dephosphorylation of Cdc37. *Mol. Cell* **31,** 886–895
11. Karnitz, L. M., and Felts, S. J. (2007) Cdc37 regulation of the kinome: when to hold 'em and when to fold 'em. *Sci. STKE* **2007,** pe22
12. Siligardi, G., Hu, B., Panaretou, B., Piper, P. W., Pearl, L. H., and Prodromou, C. (2004) Co-chaperone regulation of conformational switching in the Hsp90 ATPase cycle. *J. Biol. Chem.* **279,** 51989–51998
13. Zhao, Q., Boschelli, F., Caplan, A. J., and Arndt, K. T. (2004) Identification of a conserved sequence motif that promotes Cdc37 and cyclin D1 binding to Cdk4. *J. Biol. Chem.* **279,** 12560–12564
14. Prince, T., and Matts, R. L. (2004) Definition of protein kinase sequence motifs that trigger high affinity binding of Hsp90 and Cdc37. *J. Biol. Chem.* **279,** 39975–39981
15. Prince, T., Sun, L., and Matts, R. L. (2005) Cdk2: a genuine protein kinase client of Hsp90 and Cdc37. *Biochemistry* **44,** 15287–15295
16. Terasawa, K., Yoshimatsu, K., Iemura, S., Natsume, T., Tanaka, K., and Minami, Y. (2006) Cdc37 interacts with the glycine-rich loop of Hsp90 client kinases. *Mol. Cell. Biol.* **26,** 3378–3389
17. Polier, S., Samant, R. S., Clarke, P. A., Workman, P., Prodromou, C., and Pearl, L. H. (2013) ATP-competitive inhibitors block protein kinase recruitment to the Hsp90-Cdc37 system. *Nat. Chem. Biol.* **9,** 307–312
18. Pratt, W. B., and Toft, D. O. (1997) Steroid receptor interactions with heat shock protein and immunophilin chaperones. *Endocr. Rev.* **18,** 306–360
19. Stancato, L. F., Chow, Y. H., Hutchison, K. A., Perdew, G. H., Jove, R., and Pratt, W. B. (1993) Raf exists in a native heterocomplex with hsp90 and p50 that can be reconstituted in a cell-free system. *J. Biol. Chem.* **268,** 21711–21716
20. da Rocha Dias, S., Friedlos, F., Light, Y., Springer, C., Workman, P., and Marais, R. (2005) Activated B-RAF is an Hsp90 client protein that is targeted by the anticancer drug 17-allylamino-17-demethoxygeldanamycin. *Cancer Res.* **65,** 10686–10691
21. Phillips, J. J., Yao, Z. P., Zhang, W., McLaughlin, S., Laue, E. D., Robinson, C. V., and Jackson, S. E. (2007) Conformational dynamics of the molecular chaperone Hsp90 in complexes with a co-chaperone and anticancer drugs. *J. Mol. Biol.* **372,** 1189–1203
22. Stebbins, C. E., Russo, A. A., Schneider, C., Rosen, N., Hartl, F. U., and Pavletich, N. P. (1997) Crystal structure of an Hsp90-geldanamycin complex: targeting of a protein chaperone by an antitumor agent. *Cell* **89,** 239–250
23. Whitesell, L., and Lindquist, S. L. (2005) HSP90 and the chaperoning of cancer. *Nat. Rev. Cancer* **5,** 761–772
24. Prodromou, C., Roe, S. M., O'Brien, R., Ladbury, J. E., Piper, P. W., and Pearl, L. H. (1997) Identification and structural characterization of the ATP/ADP-binding site in the Hsp90 molecular chaperone. *Cell* **90,** 65–75
25. Lorenz, O. R., Freiburger, L., Rutz, D. A., Krause, M., Zierer, B. K., Alvira, S., Cuéllar, J., Valpuesta, J. M., Madl, T., Sattler, M., and Buchner, J. (2014) Modulation of the hsp90 chaperone cycle by a stringent client protein. *Mol. Cell* **53,** 941–953
26. Wandinger, S. K., Richter, K., and Buchner, J. (2008) The Hsp90 chaperone machinery. *J. Biol. Chem.* **283,** 18473–18477
27. Hessling, M., Richter, K., and Buchner, J. (2009) Dissection of the ATP-induced conformational cycle of the molecular chaperone Hsp90. *Nat. Struct. Mol. Biol.* **16,** 287–293
28. Xu, W., and Neckers, L. (2012) The double edge of the HSP90-CDC37 chaperone machinery: opposing determinants of kinase stability and activity. *Future Oncol.* **8,** 939–942
29. Grenert, J. P., Sullivan, W. P., Fadden, P., Haystead, T. A., Clark, J., Mimnaugh, E., Krutzsch, H., Ochel, H. J., Schulte, T. W., Sausville, E., Neckers, L. M., and Toft, D. O. (1997) The amino-terminal domain of heat shock protein 90 (hsp90) that binds geldanamycin is an ATP/ADP switch domain that regulates hsp90 conformation. *J. Biol. Chem.* **272,** 23843–23850
30. Taipale, M., Krykbaeva, I., Whitesell, L., Santagata, S., Zhang, J., Liu, Q., Gray, N. S., and Lindquist, S. (2013) Chaperones as thermodynamic sensors of drug-target interactions reveal kinase inhibitor specificities in living cells. *Nat. Biotechnol.* **31,** 630–637
31. Stancato, L. F., Silverstein, A. M., Owens-Grillo, J. K., Chow, Y. H., Jove, R., and Pratt, W. B. (1997) The hsp90-binding antibiotic geldanamycin decreases Raf levels and epidermal growth factor signaling without disrupting formation of signaling complexes or reducing the specific enzymatic activity of Raf kinase. *J. Biol. Chem.* **272,** 4013–4020
32. Eckl, J. M., Rutz, D. A., Haslbeck, V., Zierer, B. K., Reinstein, J., and Richter, K. (2013) Cdc37 (cell division cycle 37) restricts Hsp90 (heat shock protein 90) motility by interaction with N-terminal and middle domain binding sites. *J. Biol. Chem.* **288,** 16032–16042
33. Roe, S. M., Ali, M. M., Meyer, P., Vaughan, C. K., Panaretou, B., Piper, P. W., Prodromou, C., and Pearl, L. H. (2004) The mechanism of Hsp90 regulation by the protein kinase-specific cochaperone p50(cdc37). *Cell* **116,** 87–98
34. Gaiser, A. M., Brandt, F., and Richter, K. (2009) The non-canonical Hop protein from *Caenorhabditis elegans* exerts essential functions and forms binary complexes with either Hsc70 or Hsp90. *J. Mol. Biol.* **391,** 621–634
35. Eckl, J. M., Drazic, A., Rutz, D. A., and Richter, K. (2014) Nematode Sgt1-homologue D1054.3 binds open and closed conformations of Hsp90 via distinct binding sites. *Biochemistry* **53,** 2505–2514
36. Tsai, J., Lee, J. T., Wang, W., Zhang, J., Cho, H., Mamo, S., Bremer, R., Gillette, S., Kong, J., Haass, N. K., Sproesser, K., Li, L., Smalley, K. S., Fong,

D., Zhu, Y. L., Marimuthu, A., Nguyen, H., Lam, B., Liu, J., Cheung, I., Rice, J., Suzuki, Y., Luu, C., Settachatgul, C., Shellooe, R., Cantwell, J., Kim, S. H., Schlessinger, J., Zhang, K. Y., West, B. L., Powell, B., Habets, G., Zhang, C., Ibrahim, P. N., Hirth, P., Artis, D. R., Herlyn, M., and Bollag, G. (2008) Discovery of a selective inhibitor of oncogenic B-Raf kinase with potent antimelanoma activity. *Proc. Natl. Acad. Sci. U.S.A.* **105,** 3041–3046

37. Thompson, J. D., Higgins, D. G., and Gibson, T. J. (1994) CLUSTAL W: improving the sensitivity of progressive multiple sequence alignment through sequence weighting, position-specific gap penalties and weight matrix choice. *Nucleic Acids Res.* **22,** 4673–4680
38. Cole, C., Barber, J. D., and Barton, G. J. (2008) The Jpred 3 secondary structure prediction server. *Nucleic Acids Res.* **36,** W197–W201
39. Panaretou, B., Prodromou, C., Roe, S. M., O'Brien, R., Ladbury, J. E., Piper, P. W., and Pearl, L. H. (1998) ATP binding and hydrolysis are essential to the function of the Hsp90 molecular chaperone *in vivo*. *EMBO J.* **17,** 4829–4836
40. Bepperling, A., Alte, F., Kriehuber, T., Braun, N., Weinkauf, S., Groll, M., Haslbeck, M., and Buchner, J. (2012) Alternative bacterial two-component small heat shock protein systems. *Proc. Natl. Acad. Sci. U.S.A.* **109,** 20407–20412
41. Cox, J., and Mann, M. (2008) MaxQuant enables high peptide identification rates, individualized p.p.b.-range mass accuracies and proteome-wide protein quantification. *Nat. Biotechnol.* **26,** 1367–1372
42. Stafford, W. F., 3rd. (1992) Boundary analysis in sedimentation transport experiments: a procedure for obtaining sedimentation coefficient distributions using the time derivative of the concentration profile. *Anal. Biochem.* **203,** 295–301
43. Hayes, D. B., and Stafford, W. F. (2010) SEDVIEW, real-time sedimentation analysis. *Macromol. Biosci.* **10,** 731–735
44. Delaglio, F., Grzesiek, S., Vuister, G. W., Zhu, G., Pfeifer, J., and Bax, A. (1995) NMRPipe: a multidimensional spectral processing system based on UNIX pipes. *J. Biomol. NMR* **6,** 277–293
45. Vranken, W. F., Boucher, W., Stevens, T. J., Fogh, R. H., Pajon, A., Llinas, M., Ulrich, E. L., Markley, J. L., Ionides, J., and Laue, E. D. (2005) The CCPN data model for NMR spectroscopy: development of a software pipeline. *Proteins* **59,** 687–696
46. Sattler, M., Schleucher, J., and Griesinger, C. (1999) Heteronuclear multidimensional NMR experiments for the structure determination of proteins in solution employing pulsed field gradients. *Prog. Nucl. Mag. Reson. Spectrosc.* **34,** 93–158
47. Perdew, G. H., Wiegand, H., Vanden Heuvel, J. P., Mitchell, C., and Singh, S. S. (1997) A 50 kilodalton protein associated with raf and pp60(v-src) protein kinases is a mammalian homolog of the cell cycle control protein cdc37. *Biochemistry* **36,** 3600–3607
48. Zhang, W., Hirshberg, M., McLaughlin, S. H., Lazar, G. A., Grossmann, J. G., Nielsen, P. R., Sobott, F., Robinson, C. V., Jackson, S. E., and Laue, E. D. (2004) Biochemical and structural studies of the interaction of Cdc37 with Hsp90. *J. Mol. Biol.* **340,** 891–907
49. Genest, O., Reidy, M., Street, T. O., Hoskins, J. R., Camberg, J. L., Agard, D. A., Masison, D. C., and Wickner, S. (2013) Uncovering a region of heat shock protein 90 important for client binding in *E. coli* and chaperone function in yeast. *Mol. Cell* **49,** 464–473